SUPPORTING INFORMATION

Influence of the Synthetic Conditions on the Structural Diversity of Extended Manganese-Oxalato-1,2-bis(4-pyridyl)ethylene Systems

Urko García-Couceiro, Oscar Castillo,* Javier Cepeda, Mónica Lanchas, Antonio Luque, Sonia Pérez-Yáñez, Pascual Román and Daniel Vallejo-Sánchez.

Departamento de Química Inorgánica, Universidad del País Vasco, Apartado 644, E–48080 Bilbao, Spain

* Author to whom correspondence should be addressed. E-mail: oscar.castillo@ehu.es. Fax: +34 94601 35 00

S2–4. FT-IR spectra of compounds **1–5**.

S5–7. TG/DTA curves.

S8–9. Crystal structure of compound **1**.

S10–12. Crystal structure of compound **2**.

S13–15. Crystal structure of compound **3**.

S16. X-ray powder diffraction analysis of compound **1**.

S17. Variable temperature X-ray powder diffraction analysis of compound **2**.

S18. X-ray powder diffraction analysis of compound **4a**.

S19. X-ray powder diffraction analysis of compound **4b**.

S20–21. Crystal structure of compounds **5a** and **5b**.

S22. X-ray powder diffraction analysis of compound **5c**.

S23. Variable temperature X-ray powder diffraction of compound **5a**.

S24–26. Ion exchange in compounds **5a**, **5b** and **5c**.

S27. Magnetic data of compounds **1**, **5a** and **5b**

FT-IR spectra

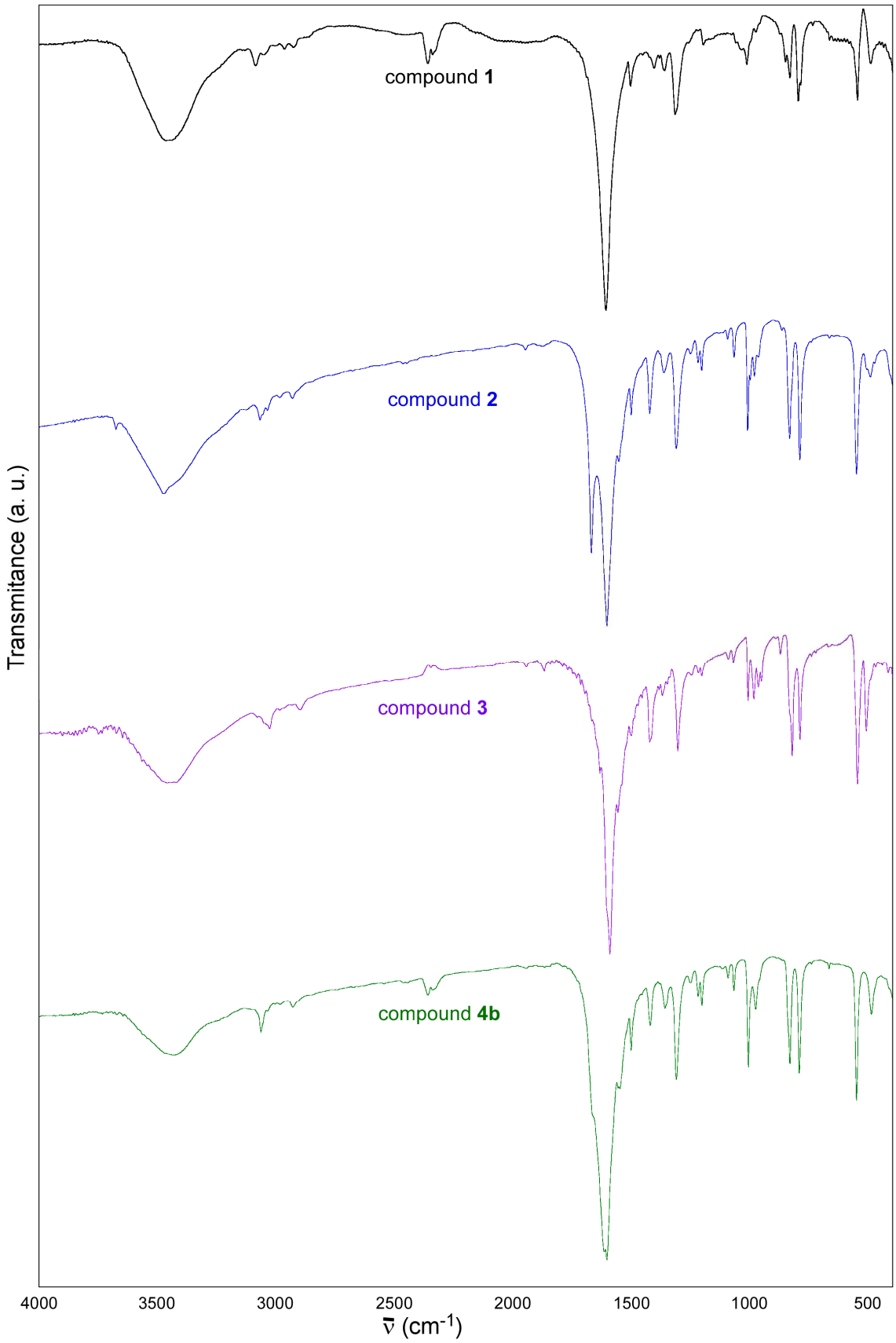

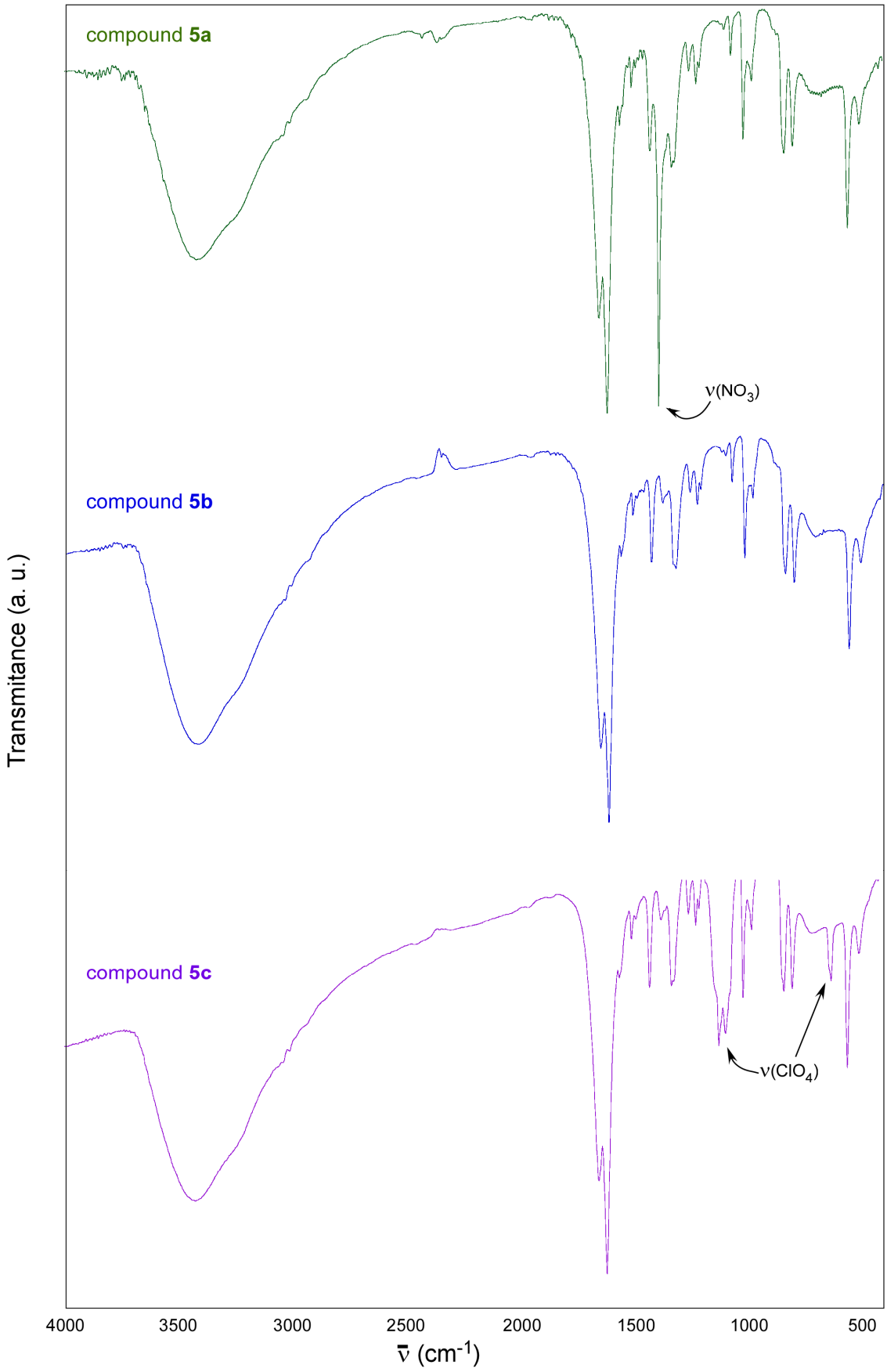
compound 5a
ν(NO3)
compound 5b
compound 5c
ν(ClO4)
Transmitance (a. u.)
4000
3500
3000
2500
2000
1500
1000
500
ν̄ (cm-1)

Table S1. IR bands (cm^{-1}) for compounds **1–4.**[a]

	1	**2**	**3**	**4b**
ν(O–H)	3455s	3475s		
ν(N–H) + ν(C–H)	3090m, 3050w, 2965w, 2930w	3070w, 3035w, 2985w, 2935w	3080w, 3030m, 2900w	3060w, 2930w
		1670vs		
ν_{as}(O–C–O)	1610vs	1605vs	1595vs	1615vs, 1605vs
ν(C–N) + ν(C–C)	1505w, 1410w,	1555w, 1505m, 1425m	1560m, 1500w, 1425w	1550w, 1500w, 1420w
ν_{s}(O–C–O)	1360w, 1320m	1365w, 1315m	1370w, 1310m	1360w, 1310m
δ_{ip}(C–H)	1200w, 1065w, 1040sh	1255w, 1220w, 1205w, 1095w, 1070w	1250w, 1220w, 1205w, 1095w, 1070w	1250w, 1220w, 1205w, 1095w, 1070w
ν_{s}(C–O)	1015m	1015m	1010m	1010m
δ_{op}(C–H) + δ_{ring}	850m, 835m	1000w, 980m, 965w, 835m	985m, 965m, 955m, 875w	980m, 835m
δ_{ip}(O–C–O)	800m, 790m	795s	825s, 790m	795m
δ_{ip}(C–C–O) + δ_{op}(O–C–O)	550m, 495m	555s, 495m	550s, 510m	555s, 490m

[a] vs = very strong, s = strong, m = medium, w = weak, sh = shoulder; ip = in plane, op = out of plane, s = symmetric, as = asymmetric.

Table S2. IR bands (cm^{-1}) for compounds **5a–5c.**[a]

	5a	**5b**	**5c**
ν(O–H)	3430vs	3430vs	3430vs
ν_{as}(O–C–O)	1650vs, 1610vs	1650vs, 1610vs	1645vs, 1610vs
ν(C–N) + ν(C–C)	1555w, 1505w, 1485w, 1425m	1560w, 1505w, 1485w, 1425m	1560w, 1505w, 1485w, 1425m
$\nu(NO_3)$	1385vs	—	—
ν_{s}(O–C–O)	1330m,	1375w, 1330m, 1315m	1375w, 1330m, 1320m
δ_{ip}(C–H)	1250w, 1225w, 1205w, 1070w	1255w, 1220w, 1205w, 1070w	1255w, 1225w, 1205w
$\nu(ClO_4)$	—	—	1120s, 1090s
ν_{s}(C–O)	1010m	1015m	1015s
δ_{op}(C–H) + δ_{ring}	980m, 835m	975m, 835m	975m, 835m
δ_{ip}(O–C–O)	795m	795m	795m
$\nu(ClO_4)$	—	—	625m
δ_{ip}(C–C–O) + δ_{op}(O–C–O)	555s, 505m	555s, 500m	555s, 500m

[a] vs = very strong, s = strong, m = medium, w = weak, sh = shoulder; ip = in plane, op = out of plane, s = symmetric, as = asymmetric.

TG-DTA curves

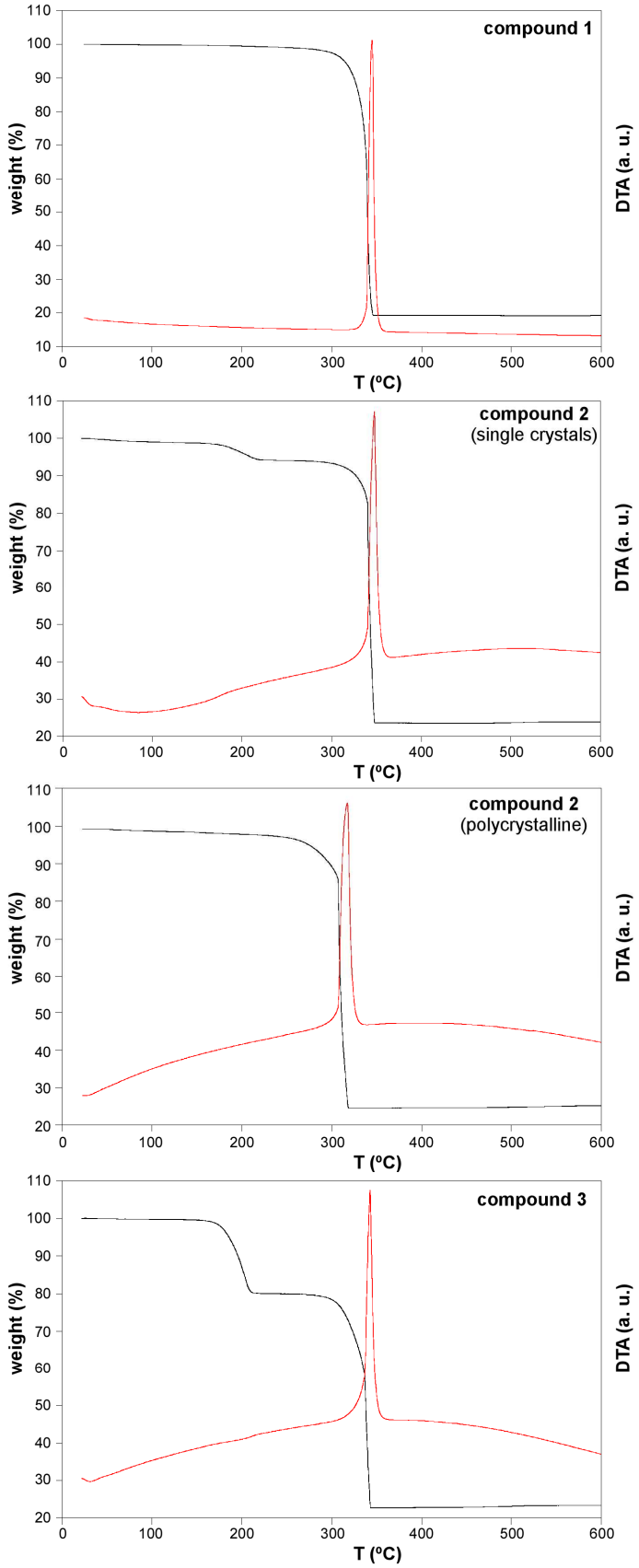

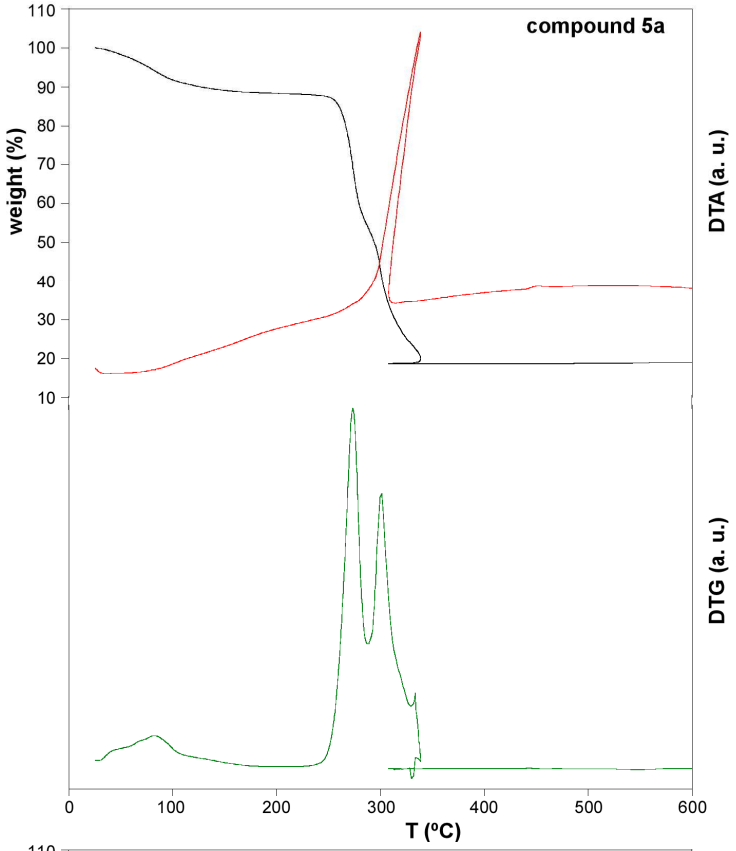
compound 5a
weight (%)
DTA (a. u.)
DTG (a. u.)
T (ºC)

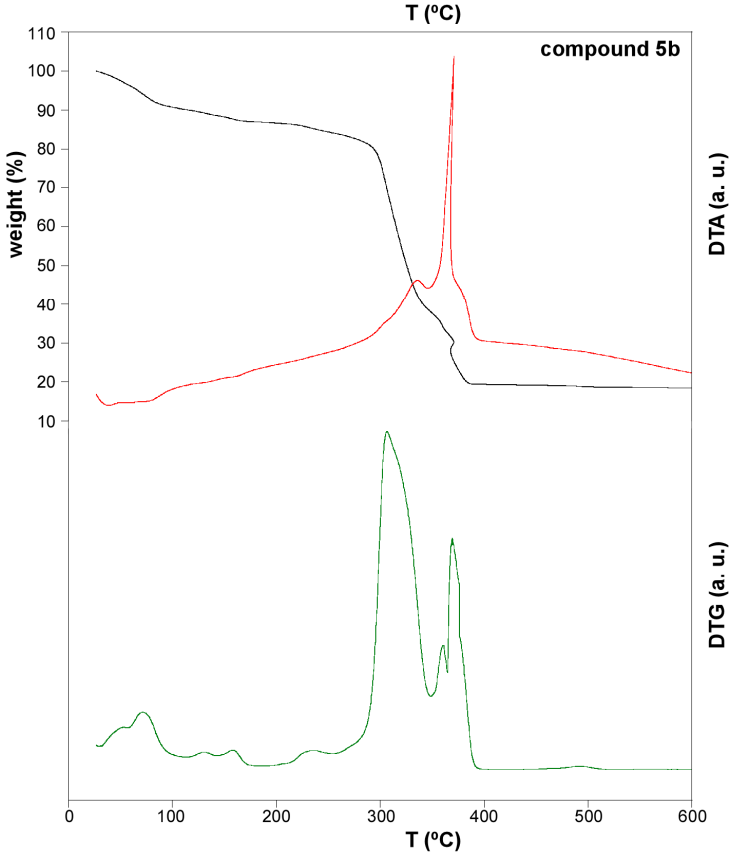
compound 5b
weight (%)
DTA (a. u.)
DTG (a. u.)
T (ºC)

Table S3. Thermal analysis data for compounds **1-3**, **5a** and **5b**.[a]

Stage	N	T_i (ºC)	T_f (ºC)	T_m (ºC)	Δm (%)	ΔH	ΣΔm (%)		Final residue
							Exp.	Teor.	
Compound 1									
1	1	300	355	345	80.70	Exo	80.70	79.88	Mn_2O_3
Compound 2 (single crystals)									
1	1	175	220	190	5.80	Exo	5.80	5.25	$–H_2O$
2	1	300	370	345	70.65	Exo	76.45	77.00	Mn_2O_3
Compound 2 (polycrystalline)									
1	1	270	340	315	75.50	Exo	75.50	75.73	Mn_2O_3
Compound 3									
1	1	170	215	200	20.20	Endo	20.20	21.89	–bpe
2	1	295	360	340	57.25	Exo	77.45	81.04	Mn_2O_3
Compound 5a									
1	1	25	160	—	11.65	Endo	11.65	11.34	$–10H_2O$
2	2	240	345	340	69.45	Exo	81.10	80.13	Mn_2O_3
Compound 5b									
1	2	25	175	—	13.20	Endo	13.20	13.14	$–5H_2O$ $–4CH_3OH$
2	3	220	395	335, 370	68.3	Exo	81.50	81.01	Mn_2O_3

[a] N = number of processes. T_i = initial temperature of the process; T_f= final temperature of the process; T_m = temperature of the maximum in the DTA curve.

Crystal structure of compound 1

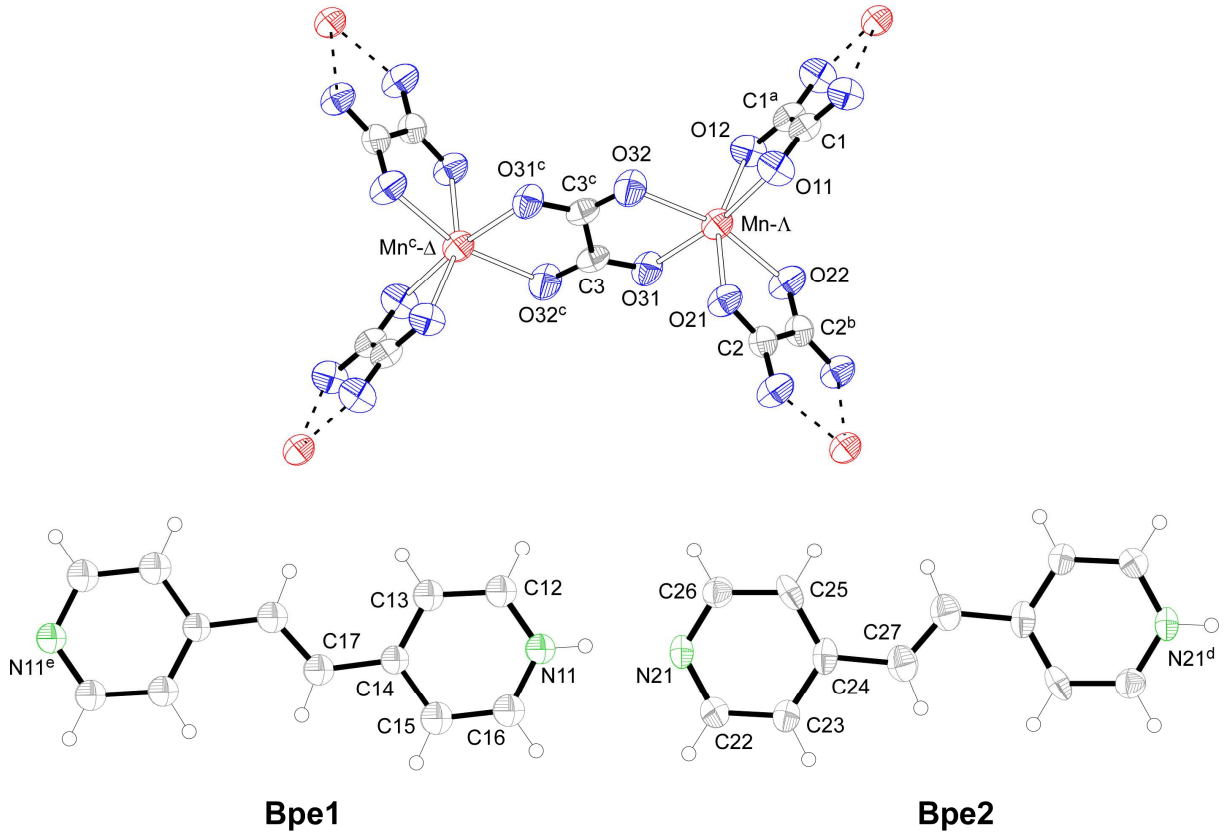

Figure S1. Manganese(II) coordination environment and the cationic bpe molecules in compound **1**. The disorder of bpe1 has been omitted for clarity. Symmetry codes: (a) 1 – x, –y, –z; (b) 1 – x, 1 – y, –z; (c) –x, 1 – y, –z; (d) 2 – x, 1 – y, 1 – z; (e) –x, –y, 1 – z.

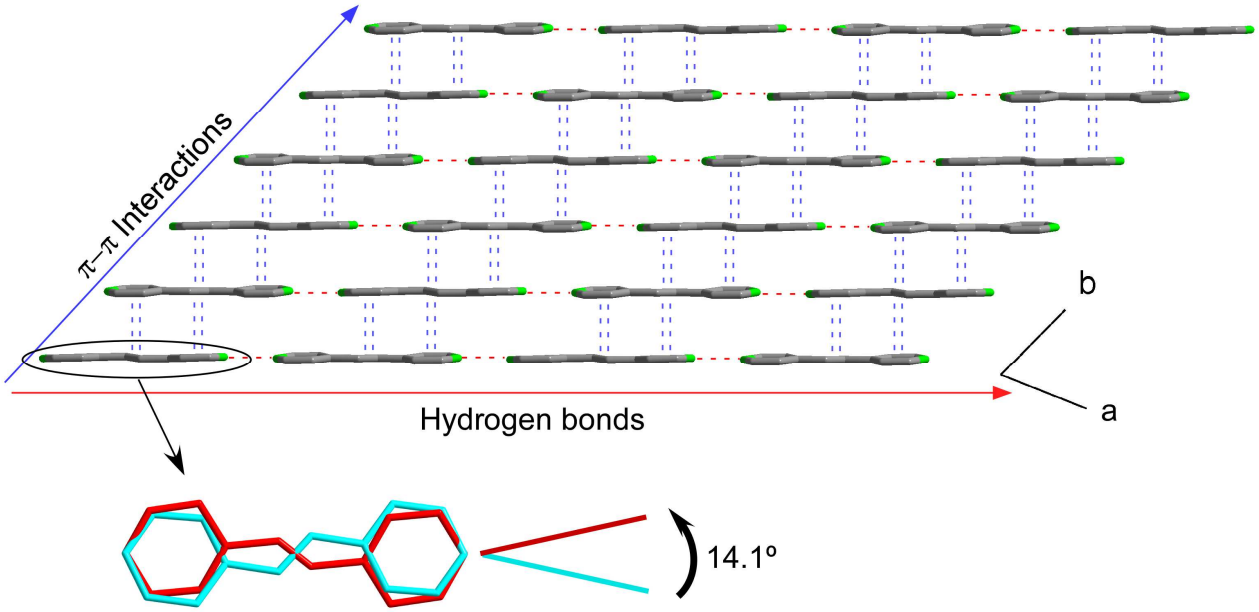

Figure S2. Packing diagram of the cationic bpe molecules showing the disorder present in bpe1 molecule in compound **1**.

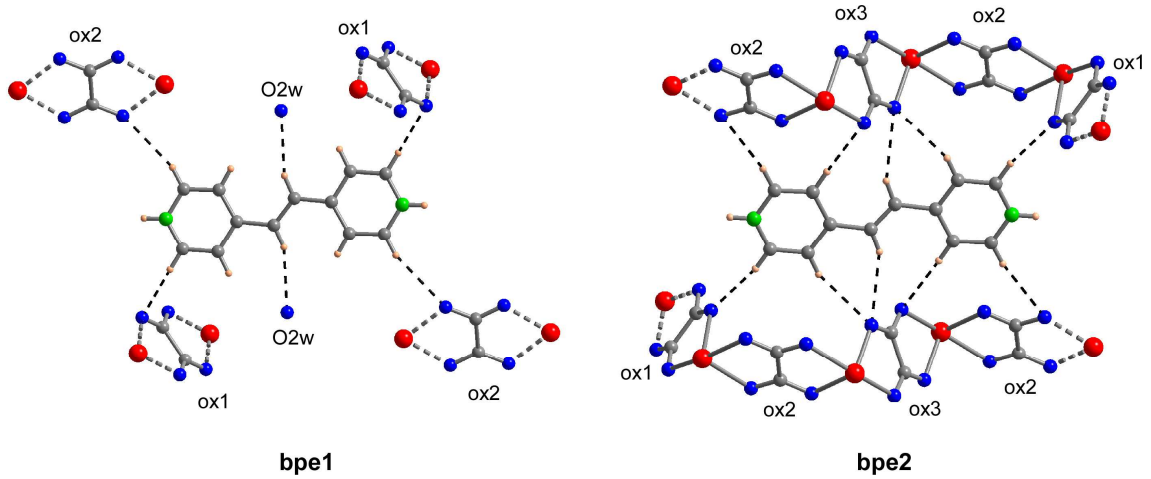

Figure S3. Hydrogen bonding interactions among the cationic bpe molecules and the anionic Mn-oxalato framework in compound **1**.

Table S4. Structural parameters of the non-covalent interactions (Å, º) in compound **1**.

D–H···A	H···A	D···A	D–H···A
Among Hbpe⁺ cations			
N11–H11···N21	1.85	2.71(1)	171
N11B–H11B···N21	1.87	2.72(2)	175
N21–H21···N11	1.85	2.71(1)	176
N21–H21···N11B	1.86	2.72(2)	180
Among Hbpe⁺ cations and $[Mn_2(ox)_3]_n^{2-}$ sheets			
C12B–H12B···O22	2.55	3.48(2)	175
C15B–H15B···O1E[a]	2.97	3.90(2)	173
C16B–H16B···O11[a]	2.51	3.41(2)	162
C17B–H17B···O1E[b]	2.84	3.75(2)	168
C12–H12···O22	2.75	3.64(1)	160
C16–H16···O11[a]	2.39	3.29(1)	161
C17–H17···O2W[c]	2.53	3.40(2)	156
C22–H22···O11[a]	2.37	3.29(1)	169
C23–H23···O31[d]	2.67	3.49(1)	146
C25–H25···O32[e]	2.68	3.59(1)	164
C26–H26···O22	2.72	3.63(1)	169
C27–H27···O31[d]	2.67	3.49(1)	148

π–π interactions among Hbpe⁺ cations[a]

Plane[b]	C=C[c]	α(º)	Dc–p (Å)	Dc-c (Å)
P1	bpe2[f]	0.5	3.35-3.36	3.39-3.42
P2	bpe2[f]	9.2	3.23-3.44	3.42-3.46
P3	bpe1[g]	1.3	3.37-3.40	3.42-3.49
P3	bpe1B[g]	3.3	3.35-3.42	3.41-3.48

Symmetry codes: (a) x, y, z + 1; (b) –x, –y, –z; (c) –x, –y, –z + 1; (d) –x + 1, –y + 1, –z + 1; (e) –x + 1, –y + 1, –z; (f) x – 1, y, z; (g) x + 1, y, z. [a] α = angle between the pyridine ring mean plane and the C=C bond. Dc–p = distance from the mean plane to the C=C carbon atoms. Dc–c = distance from the centroid of the pyridine ring to the C=C carbon atoms. [b] P1 = N11, C12, C13, C14, C15, C16; P2 = N11B, C12B, C13B, C14B, C15B, C16B; P3 = N21, C22, C23, C24, C25, C26. [c] bpe molecule involved in the non-covalent interactions established with the C=C bond.

Crystal structure of compound 2

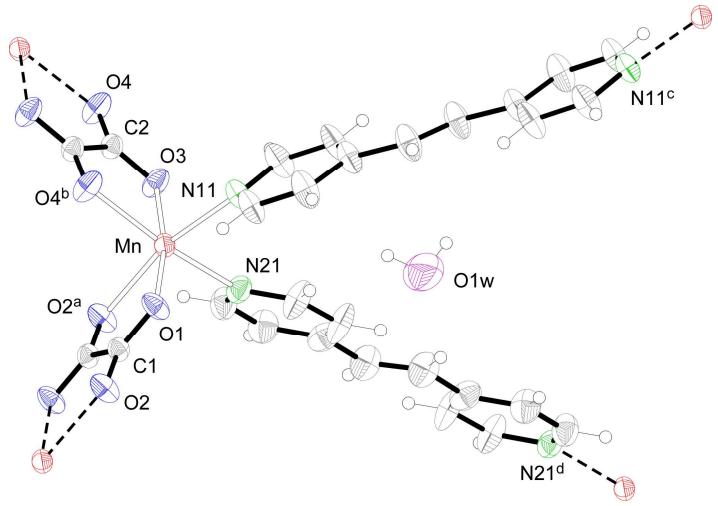

Figure S4. ORTEP of compound **2**. Symmetry codes: (a) –x, –y, –z; (b) –x, 1 – y, –z; (c) 2 – x, 1 – y, 1 – z; (d) 1 – x, – y, 1 – z.

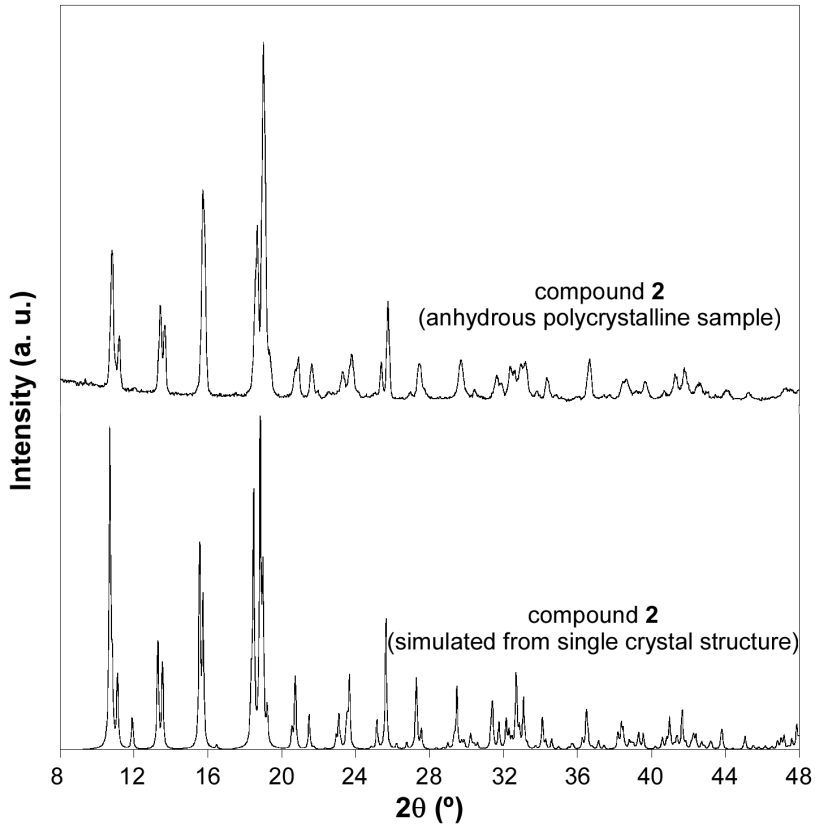

Figure S5. X-ray diffraction pattern of the anhydrous polycrystalline sample of compound **2** (above) and simulated diffractogram (below) obtained from the single-crystal X-ray structure.

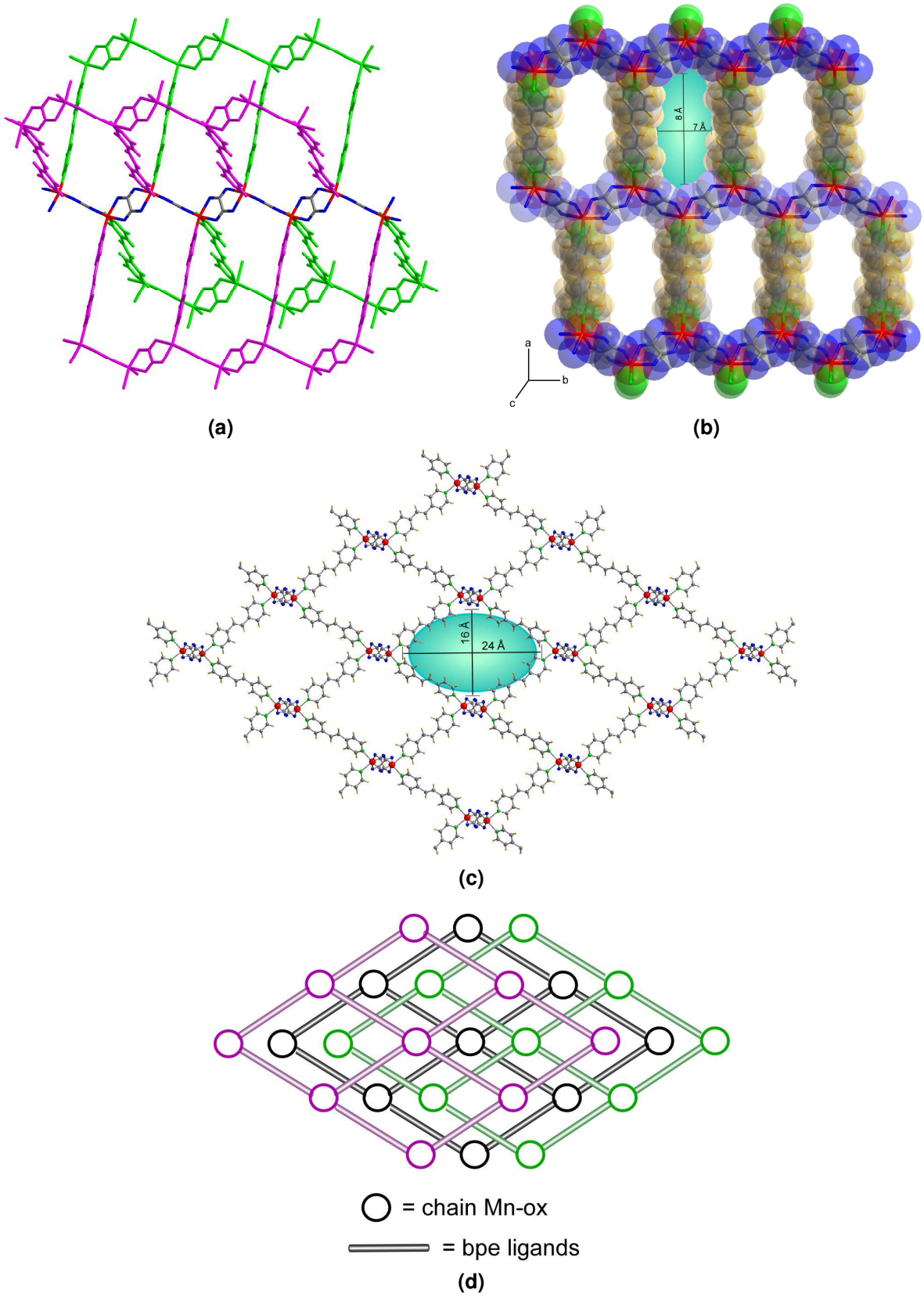

Figure S6. (a) Interconnection of each metal-oxalato backbone to surrounding four ones. (b and c) Perspective views of just one of the interpenetrating networks showing the hypothetic channels. (d) Schematic representation of the triple interpenetration.

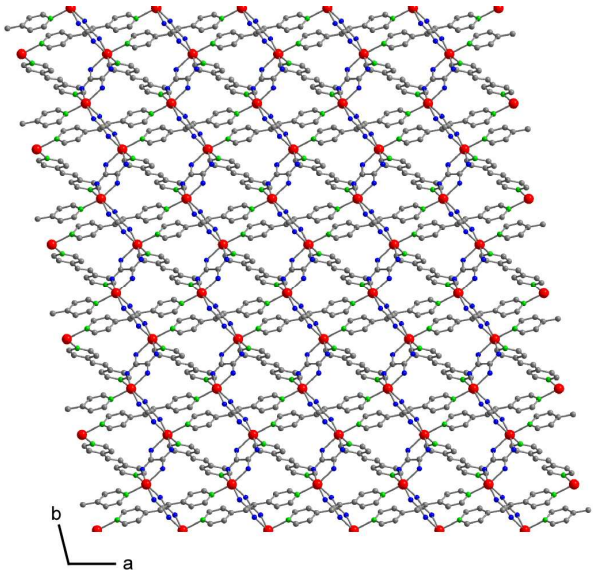

(a)

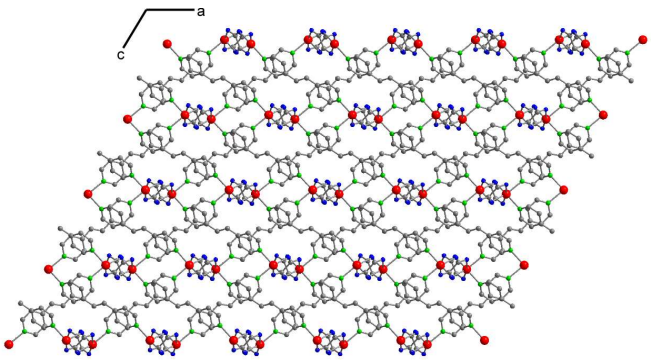

(b)

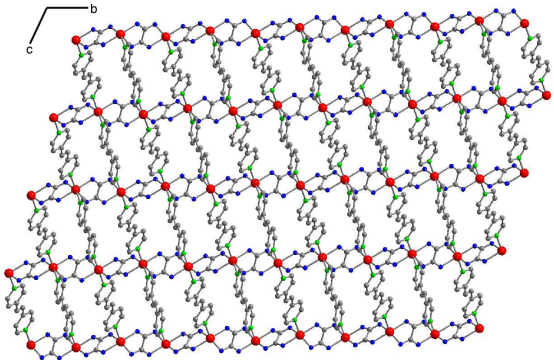

(c)

Figure S7. Perspective views of the triple interpenetrated crystal structure of compound **2**.

Table S5. Structural parameters of the non-covalent interactions (Å, º) in compound **2**.

D–H···A	**D–H**	**H···A**	**D···A**	**D–H···A**
C13–H13···O3[a]	0.93	2.54	3.400(3)	154
C17–H17···O3[b]	0.93	2.59	3.517(3)	172
C17–H17···O4[b]	0.93	2.66	3.247(3)	122
C23–H23···O2[c]	0.93	2.91	3.701(3)	144
C25–H25···O1[d]	0.93	2.60	3.460(3)	154
C27–H27···O1[c]	0.93	2.61	3.403(3)	143
C27–H27···O2[c]	0.93	2.61	3.484(3)	158
O1w–H2w···O4	0.87	2.13	2.986(10)	170
D–H···π interactions [a]				
D–H···P*i*	**D–H**	**H···C*i***	**D···C*i***	**D–H···C*i***
C26–H26···P1	0.93	3.15	3.58	134
O1w–H1w···P1	0.86	2.79	3.62	162

[a] P1: N11/C12/C13/C14/C15/C16. C*i*: centroid of the P*i* pyridine ring. Symmetry codes: (a) –x + 1, –y + 1, –z; (b) x + 1, y, z + 1; (c) x, y, z – 1; (d) –x + 1, –y, –z.

Crystal structure of compound 3

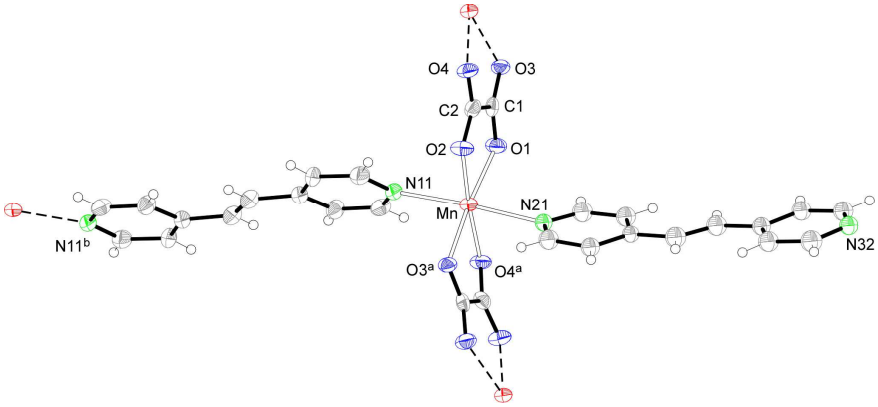

Figure S8. Ortep drawing of compound **3** showing the labelling scheme. The disorder of the terminal bpe molecule has been omitted for clarity. Symmetry codes: (a) –x + 3/2, y +1/2, –z + 1/2; (b) –x, –y, –z.

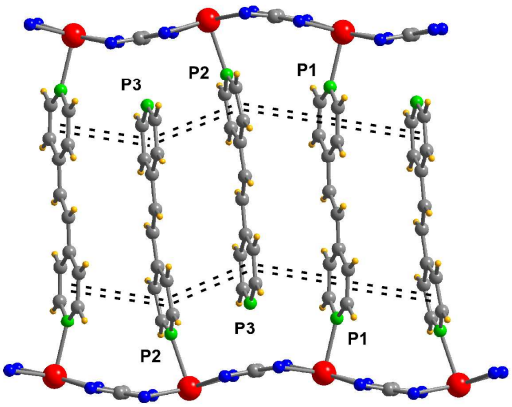

Figure S9. Non-covalent interactions established among the bpe ligands in compound **3**, showing the labelling scheme employed to denote the pyridine ring. P4 and P5 (not represented) correspond to the disordered counter partners of P2 and P3, respectively.

Table S6. Structural parameters of the π–π interactions (Å, º) in compound **3**.[a]

P*i*-P*j*[b]	Dcc (Å)	α (º)	β (º)	Dpp (Å)
P1-P2[a]	3.92(1)	10.91	24.71	1.63
P1-P3[b]	3.77(1)	5.90	30.41	1.65
P1-P4[a]	3.93(1)	13.21	26.29	1.77
P1-P5[b]	3.74(1)	5.03	27.97	1.65
P2-P3[c]	3.67(1)	7.29	21.68	1.65
P2-P5[c]	3.71(1)	6.13	24.19	1.82
P3-P4[c]	3.64(1)	9.71	25.14	1.13
P4-P5[c]	3.67(2)	8.55	20.74	1.70

[a] Dcc = centroid···centroid distances. α = dihedral angle between the rings. β = angle between the Dcc vector and normal to the first plane. Dpp = distance between the centroid of the first ring and the perpendicular projection of the centroid of the second ring on the plane of the first ring. [b] *Pi* and *Pj* being the pyridinic i/j rings of the bpe ligand. P1: N11/C12/C13/C14/C15/C16; P2: N21/C22/C23/C24/C25/C26; P3: C29/C30/C31/N32/C33/C34; P4: N21B/C22B/C23B/C24B/C25B/C26B; P5: C29B/C30B/C31B/N32B/C33B/C34B. Symmetry codes: (a) – 1/2 – x, – 1/2 + y, 1/2 – z; (b) – 3/2 + x, 1/2 – y, – 1/2 +z; (c) 1 – x, – y, 1 – z.

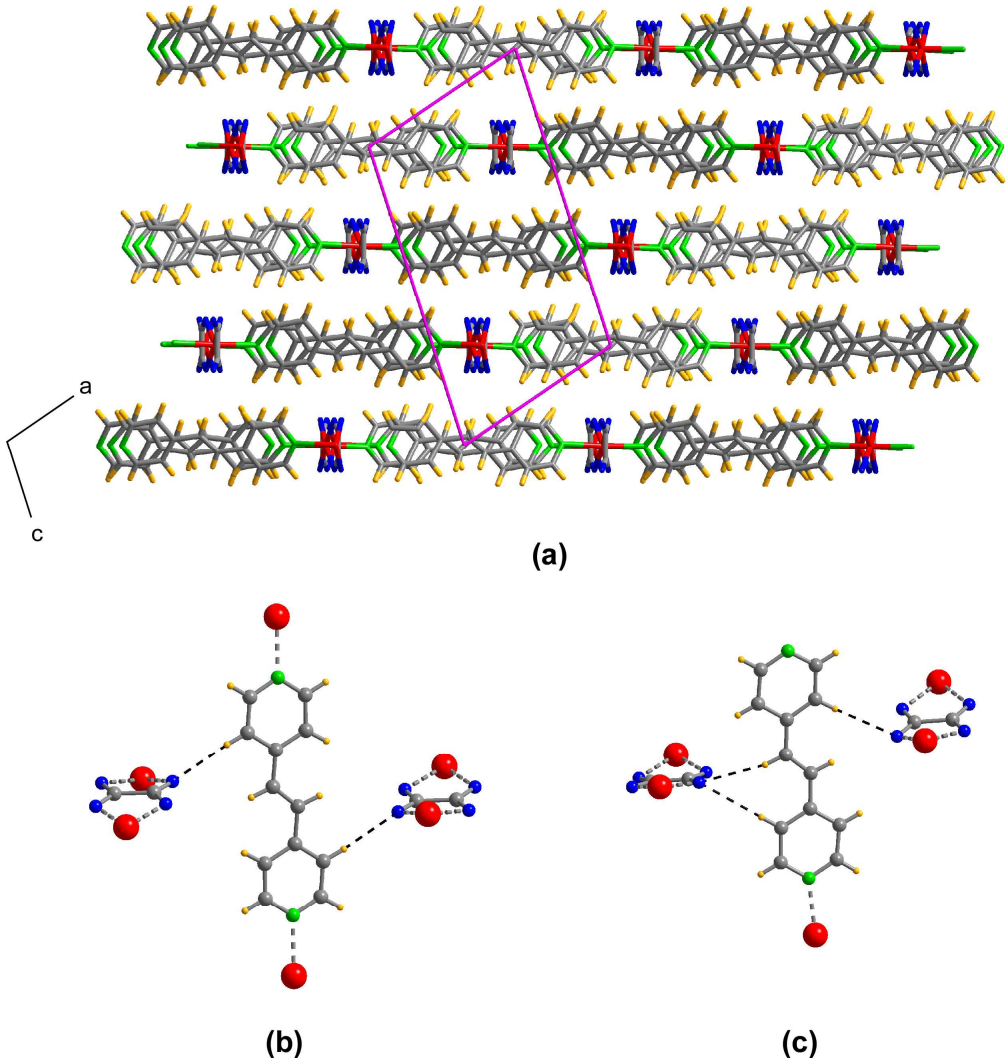

Figure S10. (a) View of the crystal packing of compound **3** along the crystallographic *b* axis. Hydrogen bonding interactions established by the bridging (b) and terminal (c) bpe ligands.

Table S7. Structural parameters of the hydrogen bonding interactions (Å, º) in compound **3**.

D–H···A	H···A	D···A	D–H···A
C15–H15···O3[a]	2.57	3.49(1)	176
C23–H23···O1[b]	2.85	3.77(1)	167
C23B–H23B···O1[b]	2.78	3.60(2)	149
C28–H28···O4[c]	2.74	3.65(1)	166
C28B–H28B···O4[b]	2.77	3.57(2)	146
C34–H34···O4[c]	2.73	3.59(1)	154
C34B–H34B···O4[c]	2.61	3.39(2)	141
C27B–H27B···O1[b]	2.73	3.61(2)	157

Symmetry codes: (a) x – 1/2, –y – 1/2, z – 1/2; (b) –x + 2, –y, –z + 1; (c) –x – 5/2, y + 1/2, –z + 1/2.

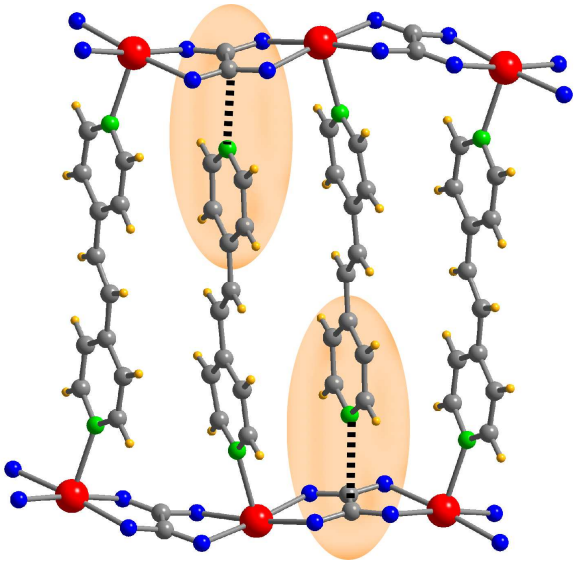

D_{N-Cent} (Å)	D_{N-C} (Å)	α (º)	β (º)
2.78 / 2.78	2.83–2.91	84.2 / 82.4	88.6 / 86.8

D_{N-Cent}: distance from the nitrogen atom to the centroid of the oxalato ligand; D_{N-C}: distance from the nitrogen atom to the carbon atoms of the oxalato ligand; α = angle between mean planes of the aromatic ring and the oxalato ligand. β = angle between the N–centroid line and the oxalato C–C bond.

Figure S11. Non-usual interaction between the aromatic ring nitrogen atom and the oxalato central C-C bond.

X-ray powder diffraction analysis of compound 1

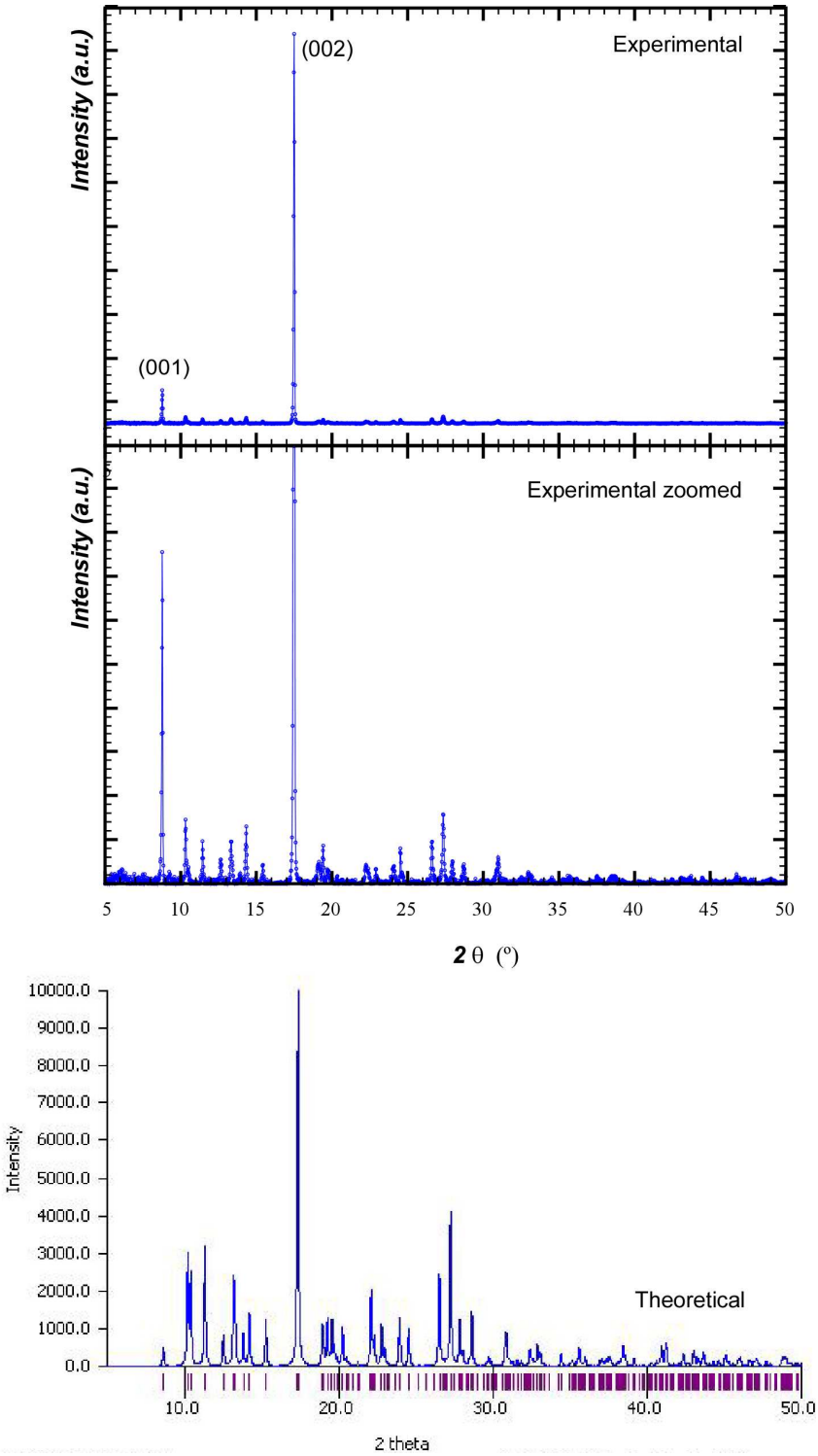

The experimental X-ray diffraction pattern (λ = 1.54056 Å) of compound **1** show an strong preferential orientation as can be observed in the figures above. Compounds with laminar crystal structure, as it is the case, usually are affected by preferential orientation.

Variable temperature X-ray powder diffraction analysis of compound 2

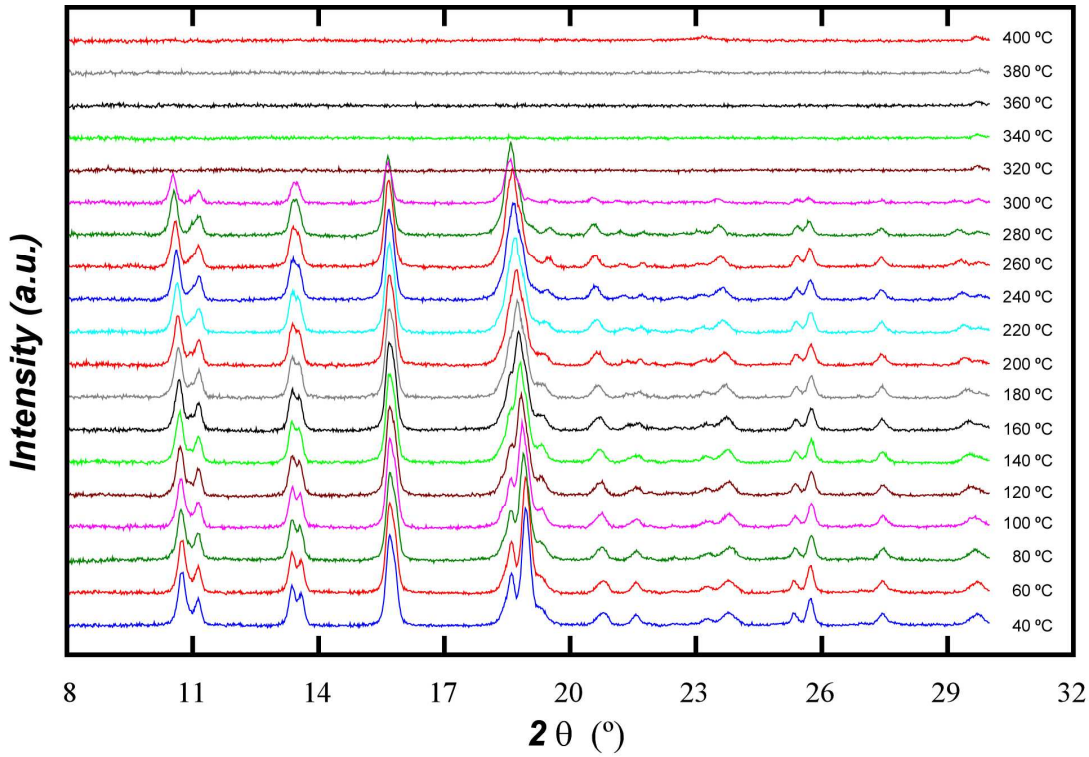

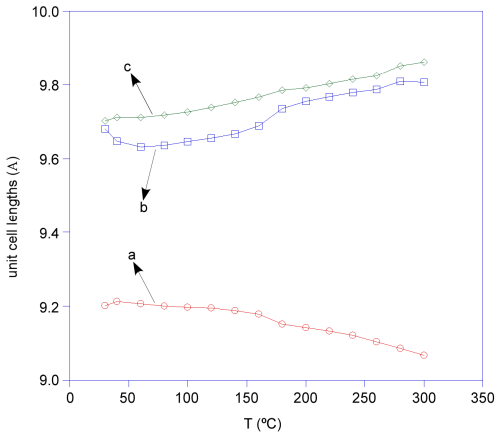

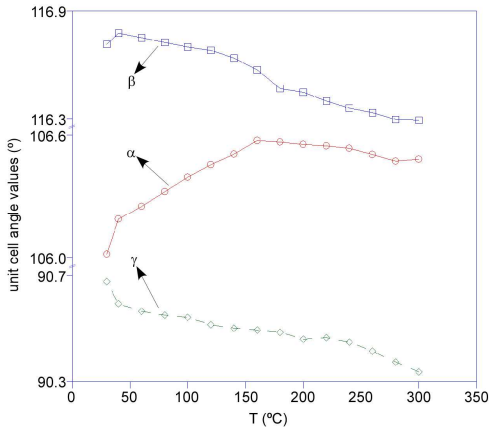

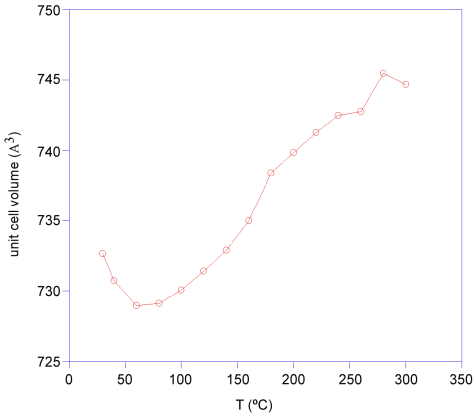

X-ray powder diffraction analysis of compound 4a

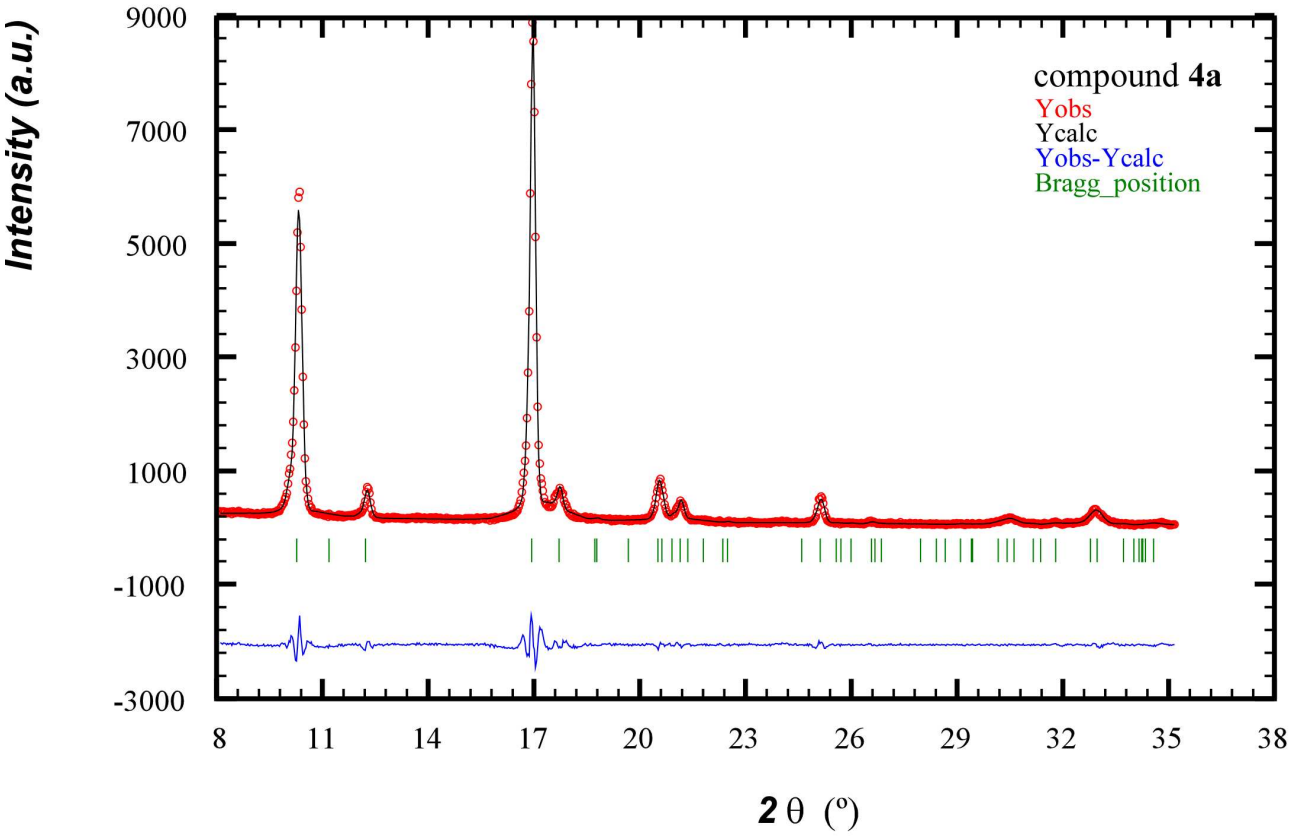

Figure S12. Final Rietveld plot for compound **4a** showing observed (dots), calculated (solid line), and difference (lower trace) powder X-ray diffraction patterns. Figures of merit: Rwp = 15.0 and Rp = 14.3.

Table S8. Crystallographic data and powder diffraction refinement details of compound **4a**.

Formula	$C_{14}H_{10}MnN_2O_4$	V (Å^3)	386.1(5)
FW (g/mol)	325.18	Z	1
Crystal System	Triclinic	$\rho_{cal.}$ (g/cm^3)	1.398
Space Group	P $\bar{1}$ *(Nº. 2)*	Colour	Yellow
a (Å)	5.311(2)	2θ range (º)	8.0–35.0
b (Å)	8.514(3)	Δ2θ (º)	0.03
c (Å)	9.224(5)	Time per step (sec.)	5
α (º)	109.96(3)	Points	1000
β (º)	94.13(2)	Parameters	13
γ (º)	97.14(4)	χ^2	2.95

X-ray powder diffraction analysis of compound 4b

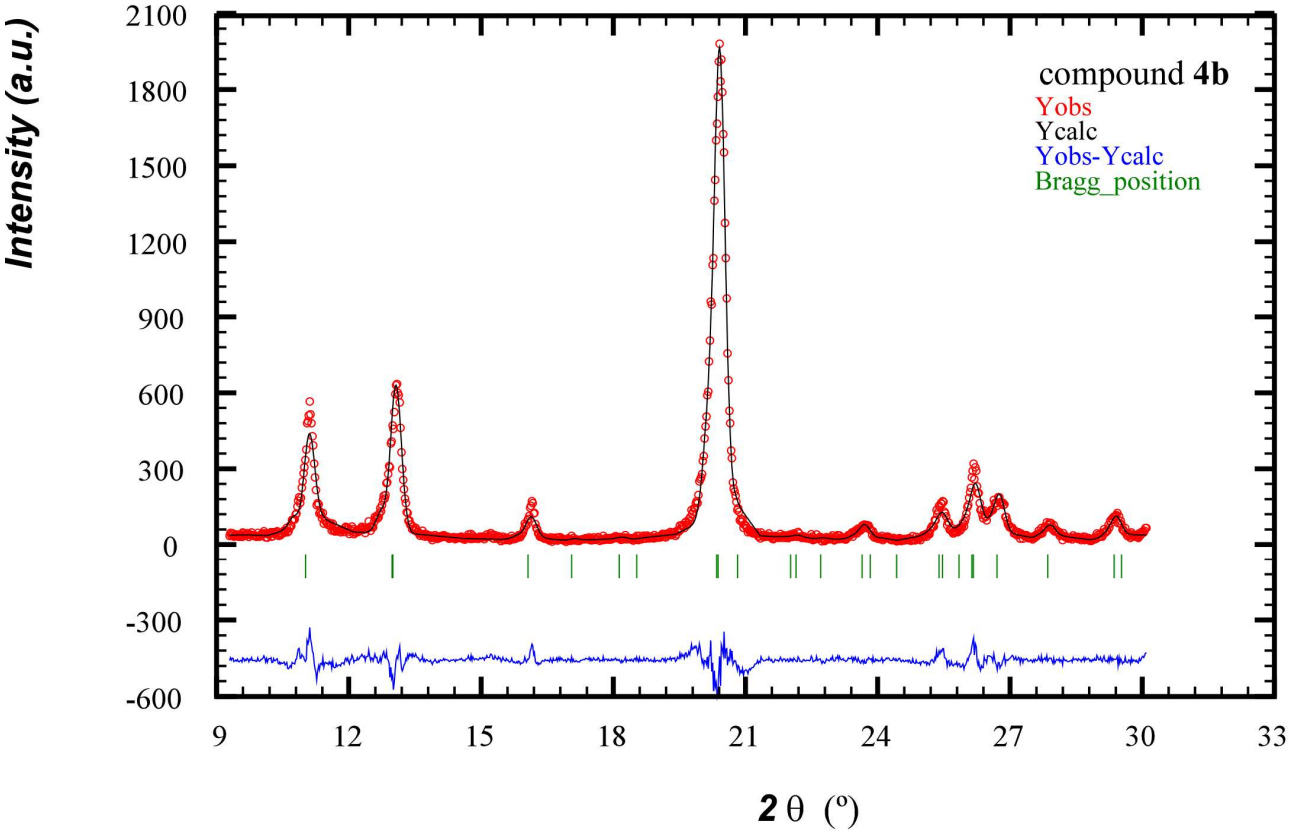

Figure S13. Final Rietveld plot for compound **4b** showing observed (dots), calculated (solid line), and difference (lower trace) powder X-ray diffraction patterns. Figures of merit: Rwp = 24.3 and Rp = 19.9.

Table S9. Crystallographic data and powder diffraction refinement details of compound **4b**.

Formula	$C_{14}H_{10}MnN_2O_4$	V (Å^3)	351.8(4)
FW (g/mol)	325.18	Z	1
Crystal System	Triclinic	$\rho_{cal.}$ (g/cm^3)	1.534
Space Group	P $\bar{1}$ *(Nº. 2)*	Colour	Yellow
a (Å)	5.833(5)	2θ range (º)	9.0–30.0
b (Å)	7.872(5)	Δ2θ (º)	0.02
c (Å)	8.854(5)	Time per step (sec.)	5
α (º)	113.68(2)	Points	1051
β (º)	90.49(3)	Parameters	12
γ (º)	107.20(7)	χ^2	2.94

Crystal structure of compounds 5a and 5b

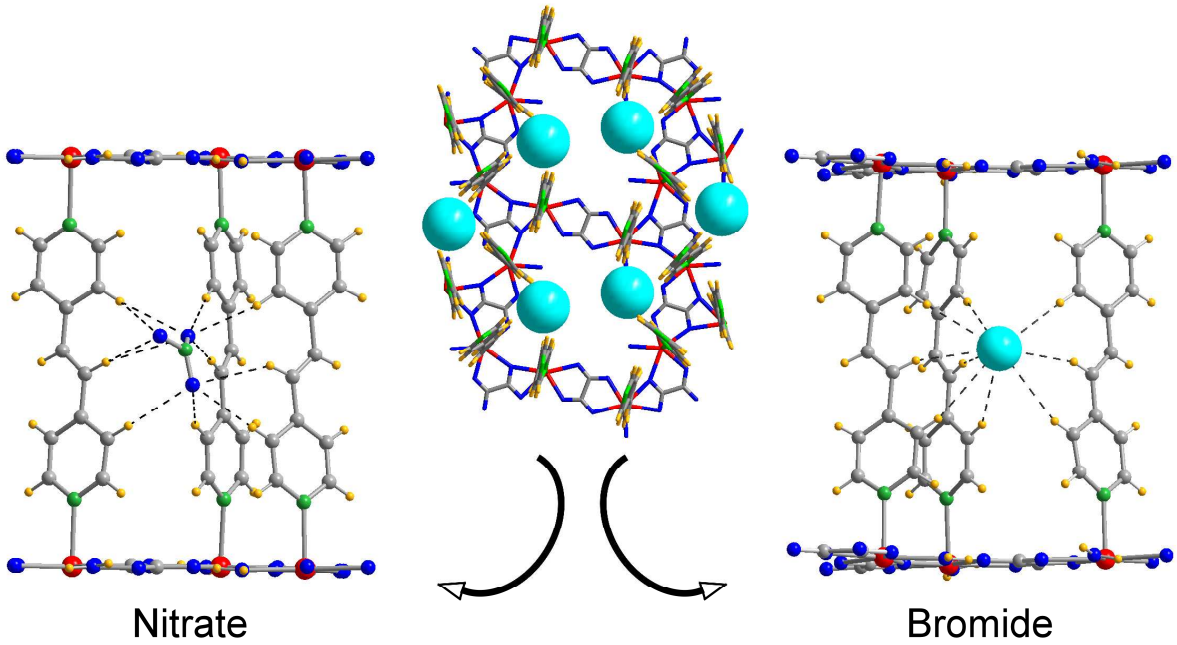

Figure S14. Anchoring of the counterions into the 3D crystal structure of compounds **5a** and **5b**. Only one of the two disordered nitrate anions has been represented for clarity.

Table S10. Structural parameters of the hydrogen bonding interactions (Å, º) in compound **5a**.

D–H···A	H···A (Å)	D···A (Å)	D–H···A (º)
O1w–H12w···O12	2.08	2.714(3)	130
O1w–H12w···O32	2.00	2.694(3)	138
O2w–H21w···O21[a]	2.74	3.594(3)	176
Nitrate 1 (54%)			
C13–H13···O53[b]	2.89	3.76(1)	156
C15–H15···O51[c]	2.72	3.56(1)	152
C15–H15···O52[c]	2.58	3.48(1)	162
C17–H17···O52[b]	2.50	3.42(1)	174
C18–H18···O51	2.68	3.60(1)	169
C18–H18···O52	2.90	3.71(1)	146
C20–H20···O52[d]	2.50	3.43(1)	177
C24–H24···O53	2.60	3.49(2)	161
C33–H33···O52[e]	2.53	3.40(1)	156
C38–H38···O53[a]	2.86	3.64(1)	143
C40–H40···O53[a]	2.46	3.31(1)	152
Nitrate 2 (46%)			
C13–H13···O62[b]	2.51	3.36(1)	152
C15–H15···O61[c]	2.47	3.35(1)	159
C17–H17···O62[b]	2.66	3.49(2)	148
C18–H18···O62	2.85	3.62(1)	140
C24–H24···O62	2.87	3.64(1)	140
C33–H33···N6[e]	2.67	3.60(2)	176
C38–H38···O63[a]	2.81	3.69(2)	159
C38–H38···O62[a]	2.67	3.47(1)	144

Symmetry codes: (a) x, y + 1, z; (b) –x – 2, y + 1/2, –z + 1/2; (c) x – 1, y, z; (d) –x – 1, y + 1/2, –z + 1/2; (e) x – 1, y + 1, z.

Table S11. Structural parameters of the hydrogen bonding interactions (Å, º) in compound **5b**.

D–H···A	H···A (Å)	D···A (Å)	D–H···A (º)
O1w–H12w···O12	2.26	2.748(6)	116
O1w–H12w···O32	2.07	2.710(6)	130
O2w–H21w···O21[a]	2.79	3.644(6)	171
C13–H13···Br[b]	3.35	4.190(8)	151
C15–H15···Br[c]	3.11	4.044(9)	178
C17–H17···Br[b]	3.23	4.104(10)	157
C18–H18···Br	2.91	3.796(10)	160
C20–H20···Br[d]	3.55	4.478(9)	176
C24–H24···Br	3.23	4.046(8)	148
C33–H33···Br[e]	3.04	3.971(10)	176
C38–H38···Br[a]	2.90	3.786(14)	159
C40–H40···Br[a]	3.34	4.139(11)	145

Symmetry codes: (a) x, y + 1, z; (b) –x – 2, y + 1/2, –z + 1/2; (c) x – 1, y, z; (d) –x – 1, y + 1/2, –z + 1/2; (e) x – 1, y + 1, z.

X-ray powder diffraction analysis of compound 5c

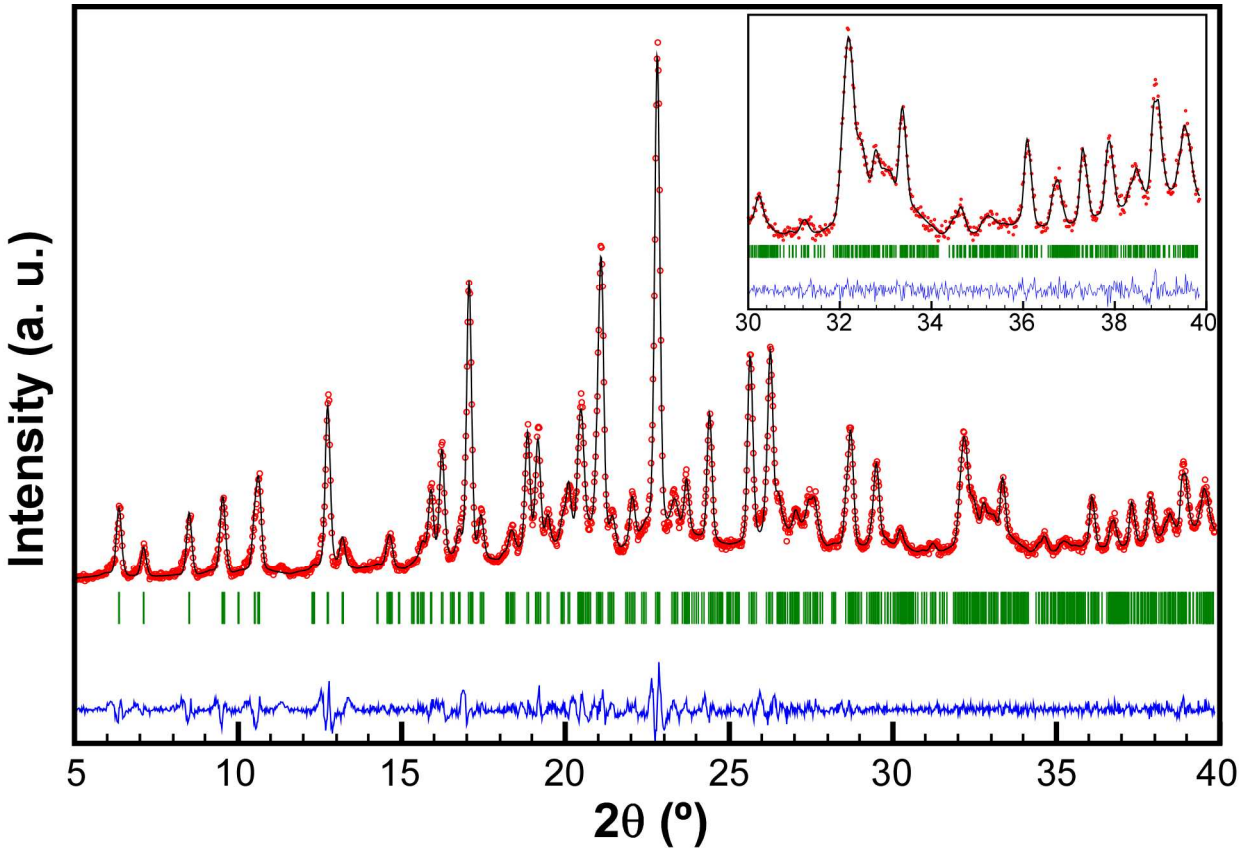

Figure S15. Final Rietveld plot for compound **5c** showing observed (dots), calculated (solid line), and difference (lower trace) powder X-ray diffraction patterns. Figures of merit: Rwp = 16.3 and Rp = 14.5.

Table S12. Crystallographic data and powder diffraction refinement details of compound **5c**.

Formula	$C_{27}H_{24}Cl_1Mn_2N_5O_{11}$	Z	4
FW (g/mol)	704.39	$\rho_{cal.}$ (g/cm^3)	1.245
Crystal System	Monoclinic	Colour	Yellow
Space Group	$P2_1/c$ *(Nº. 14)*	2θ range (º)	5.0–40.0
a (Å)	13.899(1)	Δ2θ (º)	0.02
b (Å)	11.444(1)	Time per step (sec.)	4
c (Å)	24.860(2)	Points	1751
β (º)	90.32(1)	Parameters	8
V (Å^3)	3954.2(5)	χ^2	3.19

Variable-temperature X-ray powder diffraction of compound 5a

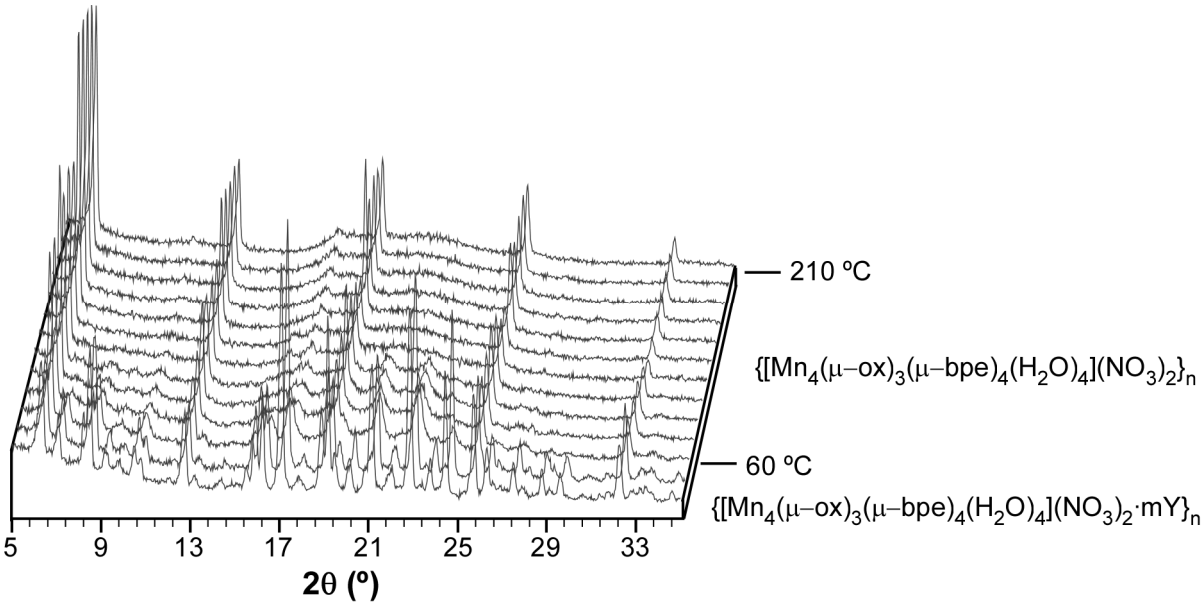

Figure S16. Variable-temperature X-ray powder diffraction measurements of compound **5a,** showing the collapse of the crystal structure during the release of the inclusion solvent molecules.

Ion exchange in compounds 5a, 5b and 5c

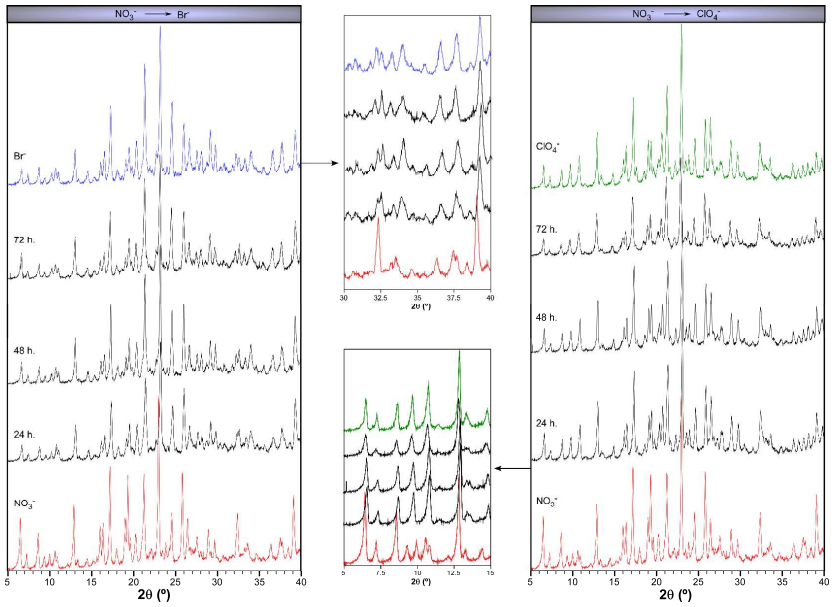

Figure S17. Diffraction patterns performed during the ion exchange experiments on compound **5a** (NO_3^-, red line). Compound **5b** (Br^-, blue line) and compound **5c** (ClO_4^-, green line).

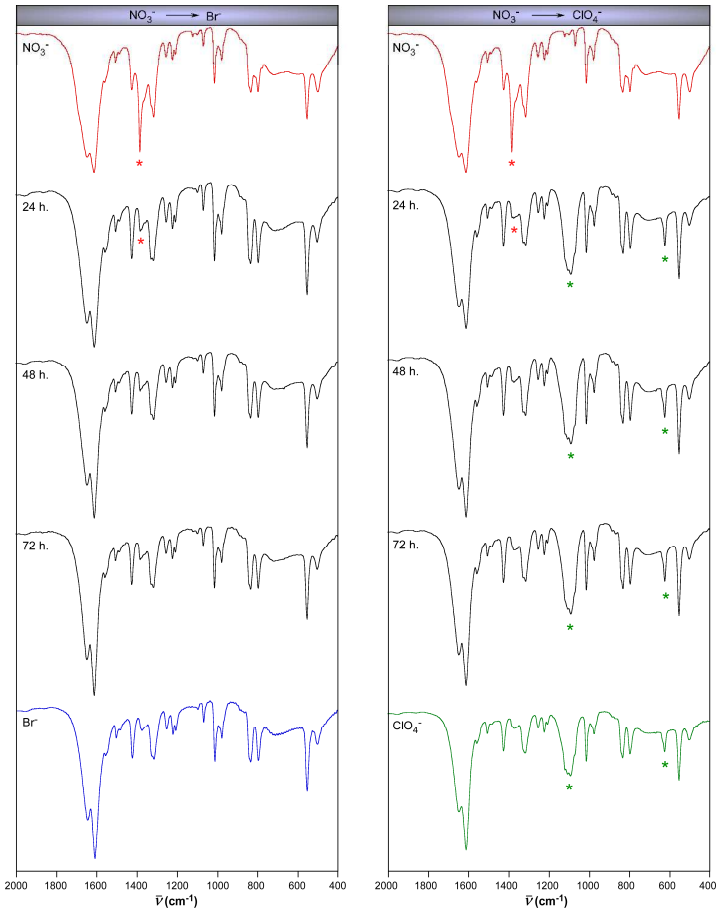

Figure S18. IR spectra performed during the ion exchange experiments on compound **5a** (NO_3^-, red line). Compound **5b** (Br^-, blue line) and compound **5c** (ClO_4^-, green line). Asterisks indicate the most characteristic bands for each anion.

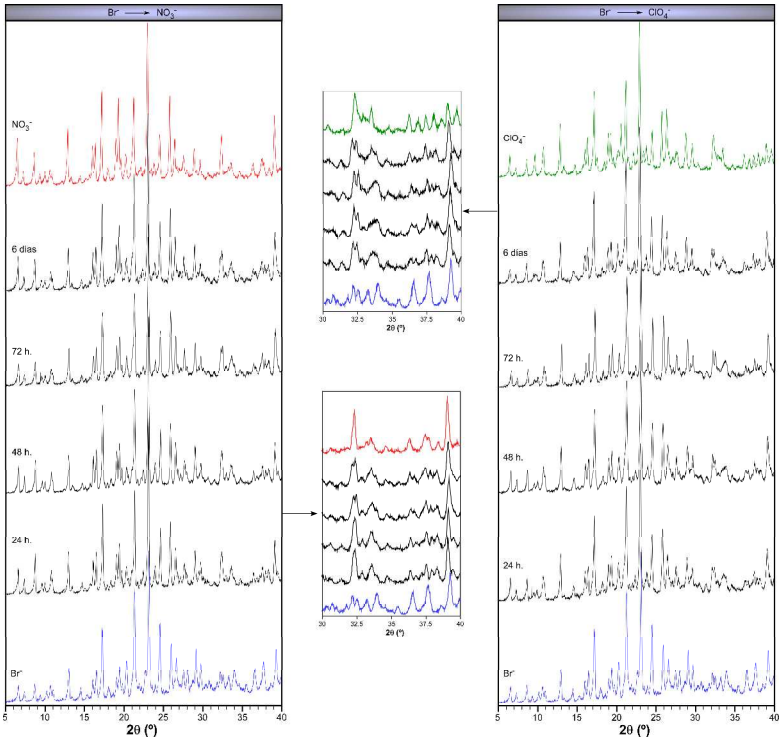

Figure S19. Diffraction patterns performed during the ion exchange experiments on compound **5b** (Br^-, blue line). Compound **5a** (NO_3^-, red line) and compound **5c** (ClO_4^-, green line).

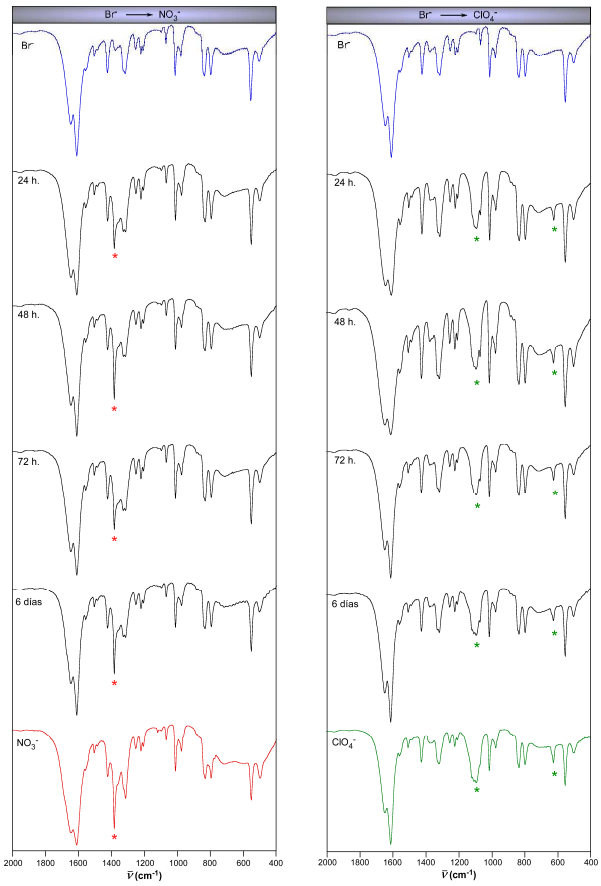

Figure S20. IR spectra performed during the ion exchange experiments on compound **5b** (Br^-, blue line). Compound **5a** (NO_3^-, red line) and compound **5c** (ClO_4^-, green line). Asterisks indicate the most characteristic bands for each anion.

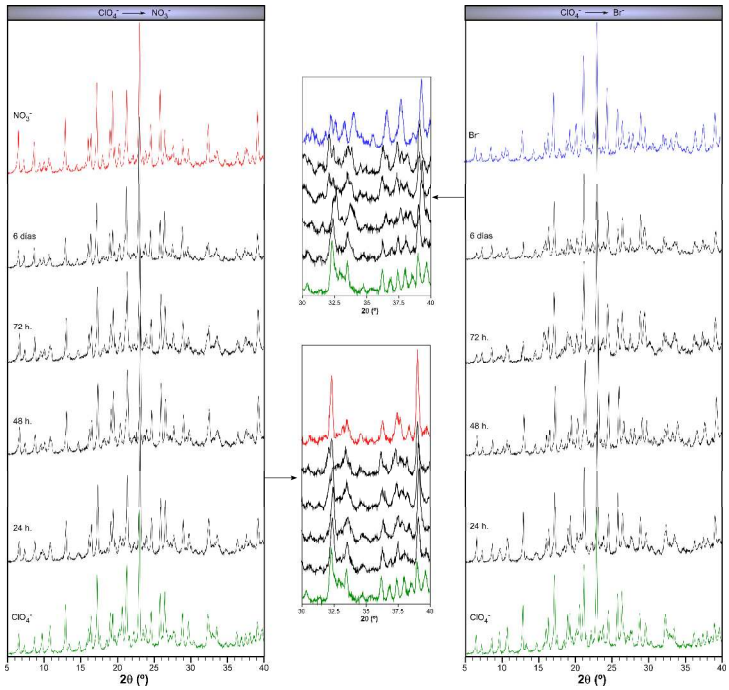

Figure S21. Diffraction patterns performed during the ion exchange experiments on compound **5c** (ClO_4^-, green line). Compound **5a** (NO_3^-, red line) and compound **5b** (Br^-, blue line).

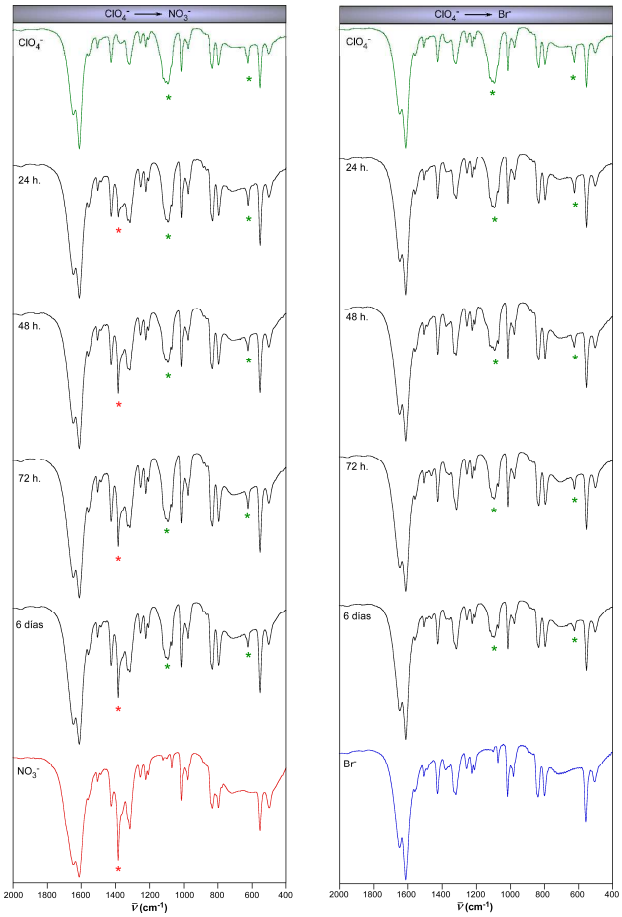

Figure S22. IR spectra performed during the ion exchange experiments on compound **5c** (ClO_4^-, green line). Compound **5a** (NO_3^-, red line) and compound **5b** (Br^-, blue line). Asterisks indicate the most characteristic bands for each anion.

Magnetic data of compounds 1, 5a and 5b

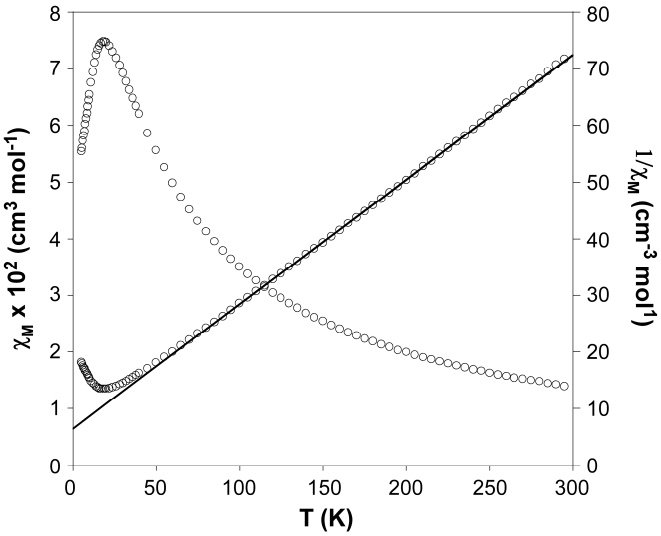

Figure S23. Thermal dependence of χ_M and $1/\chi_M$ for compound **1**. The solid line represents the best fit for the Curie-Weiss law.

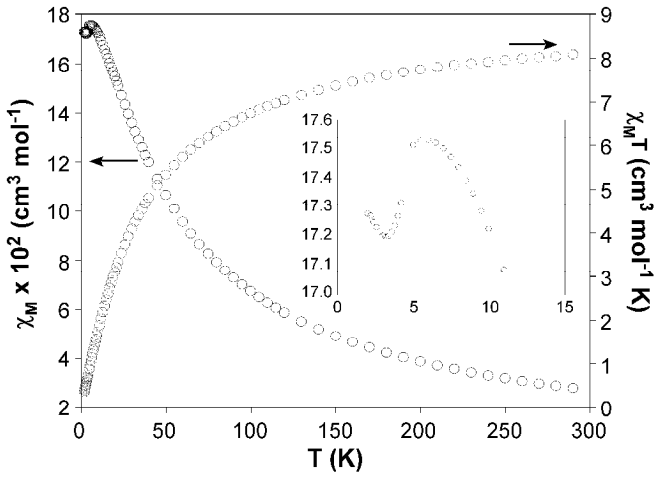

Figure S24. Thermal dependence of χ_M and χ_MT for compound **5a**.

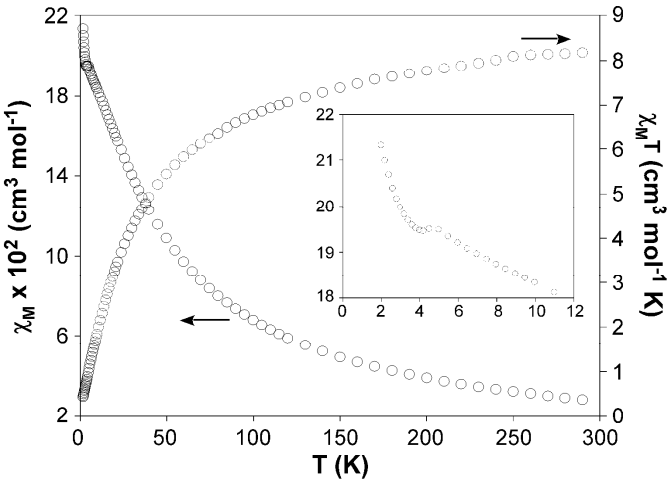

Figure S25. Thermal dependence of χ_M and χ_MT for compound **5b**.